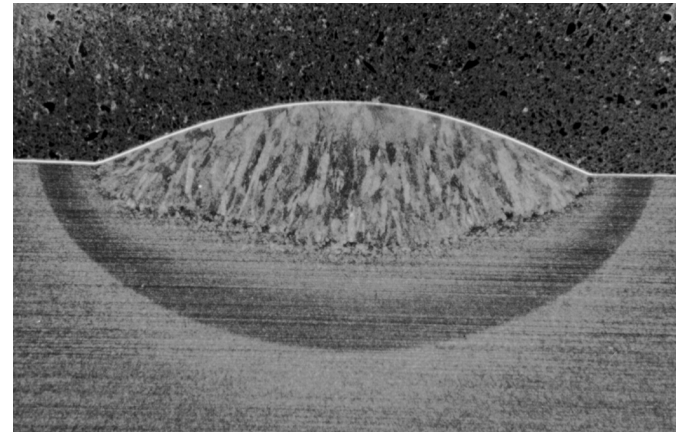
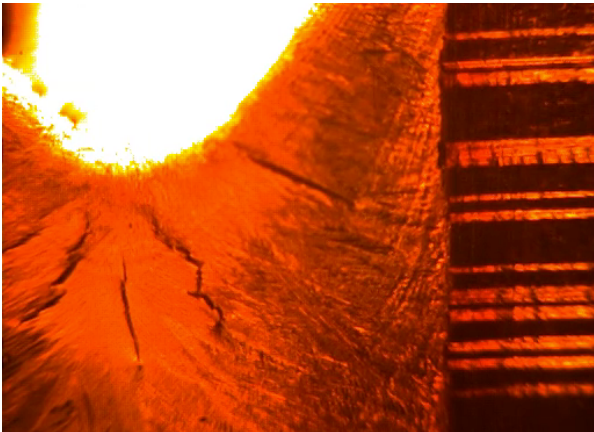
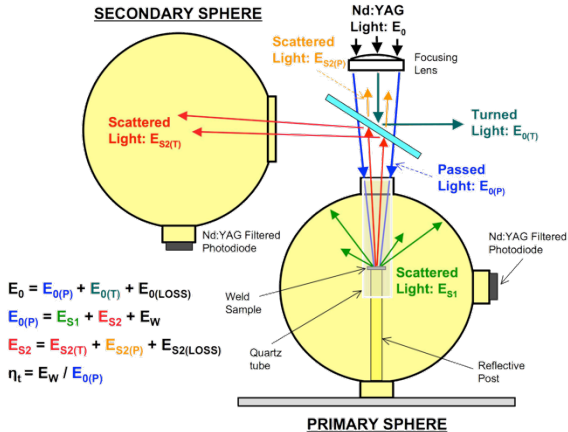


Exceptional service in the national interest



Engineering Approximations in Welding

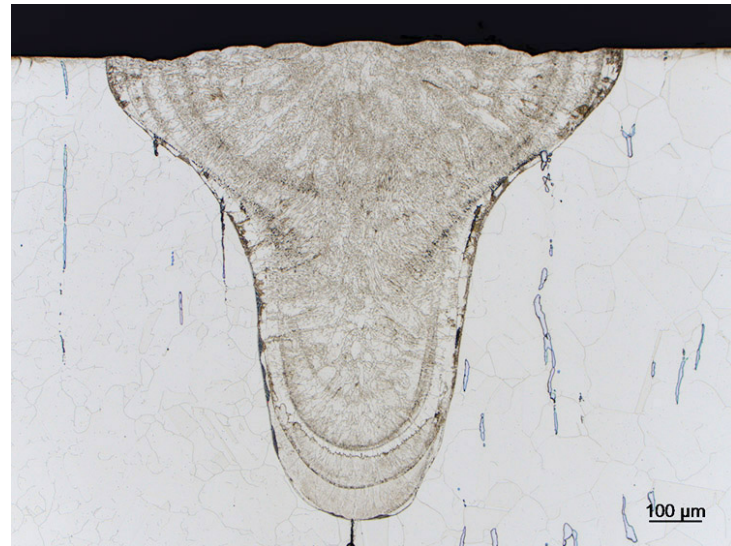
Bridging the Gap Between the Speculation and Simulation

C.V. Robino

November 9, 2015

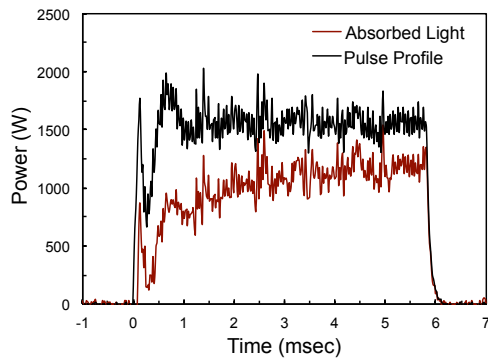
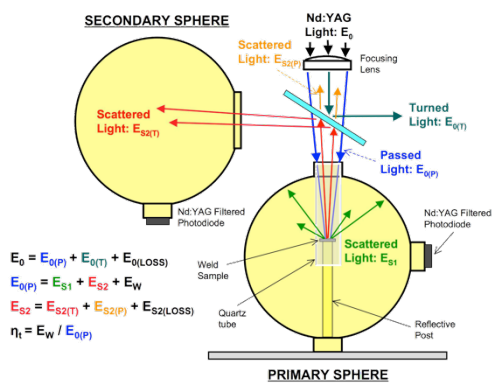
Introduction

- Welding engineers and metallurgists are often confronted with questions we don't know the answers to:
 - *"We need to make a laser spot weld next to an extremely heat sensitive component – will welding damage it"*
 - *"We going to make this assembly out of an alloy we've never welded before – will the welds crack"*
 - *"We'd like to use this new alloy to make a welded structural part for a one-off test – will it be strong enough"*
- There usually isn't time for full up welding trials or simulations, and guessing is never a satisfying or reliable option
- All of us have developed tools to address these situations

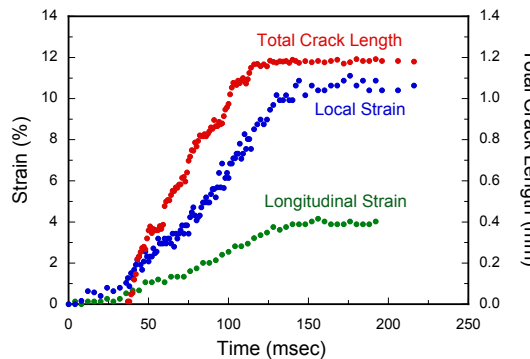
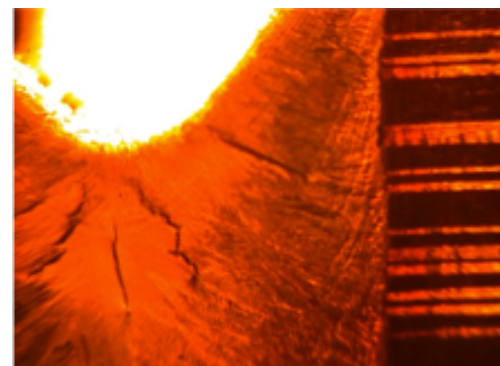


Some examples

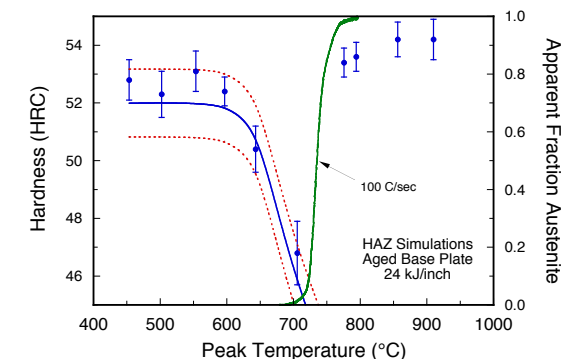
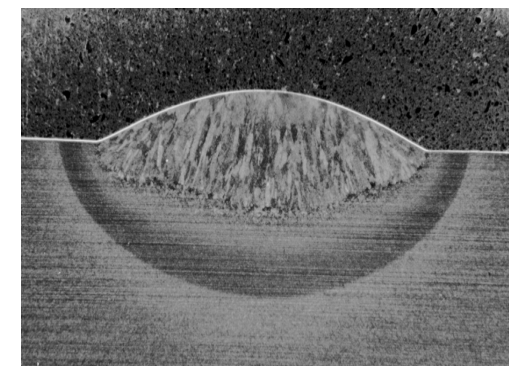
- Energy absorption in pulsed laser welds



- Dynamics of weld hot cracking

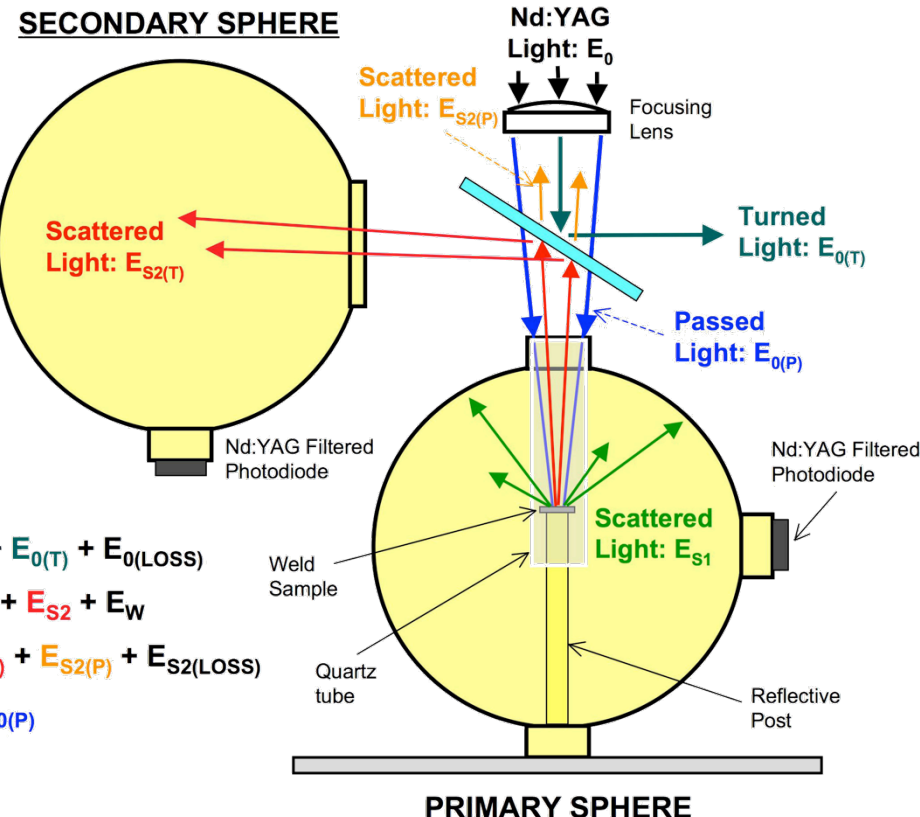


- HAZ softening in a high strength steel

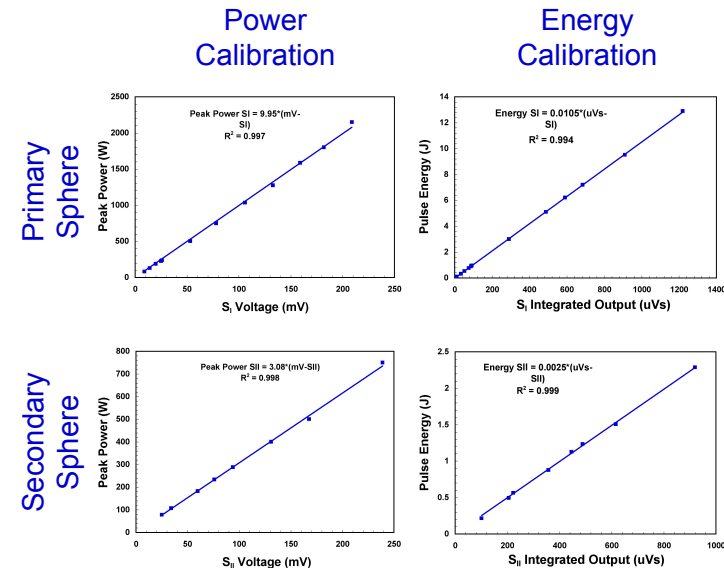


Energy absorption in pulsed laser welds

- Understanding energy transfer is critical for estimating welding temperatures and process optimization
- Basic concept: Capture and measure the reflected light by welding inside an integrating sphere

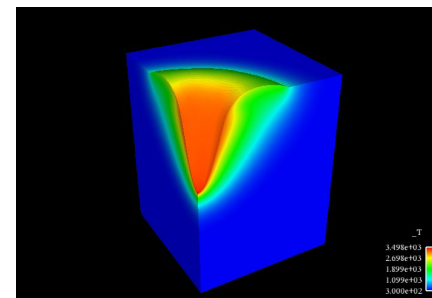
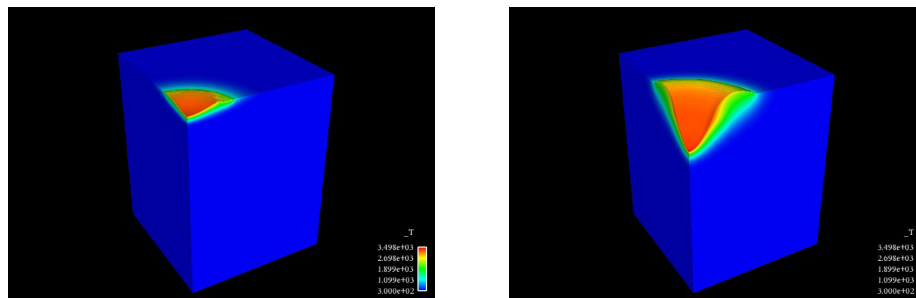
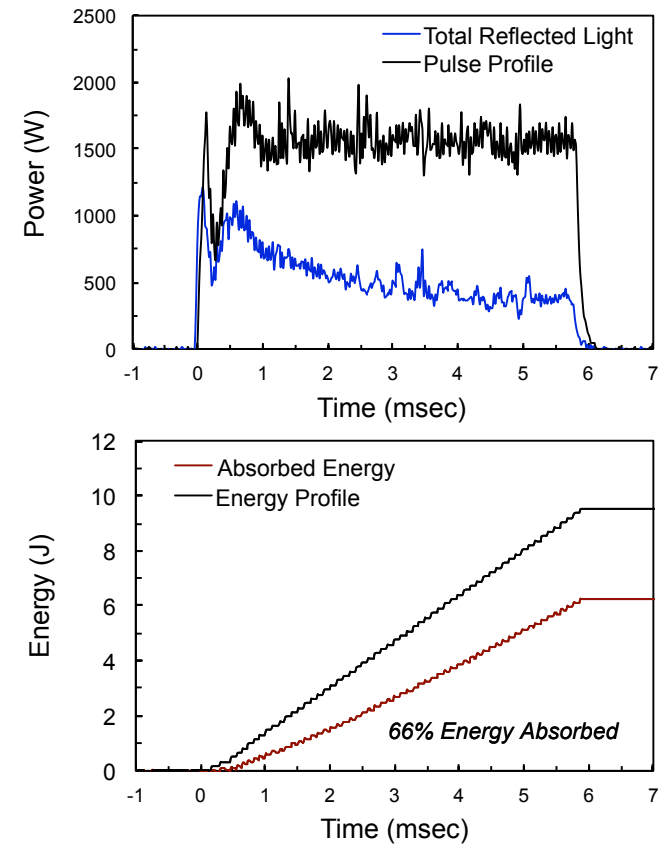
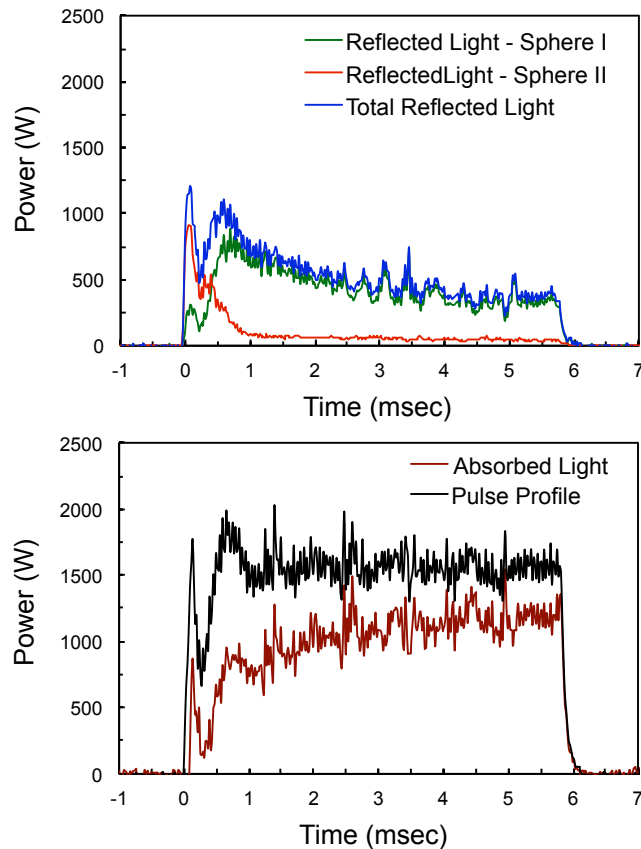


- Method requires rigorous characterization and calibrations

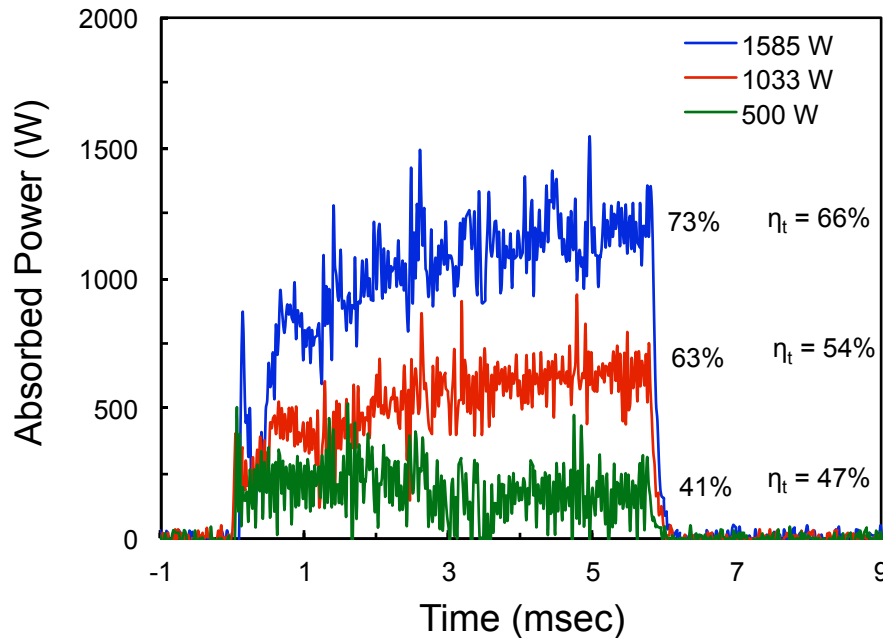


Results and phenomenology

- Initial reflection is high as melting and keyhole are established
- Absorption increases and ultimately saturates



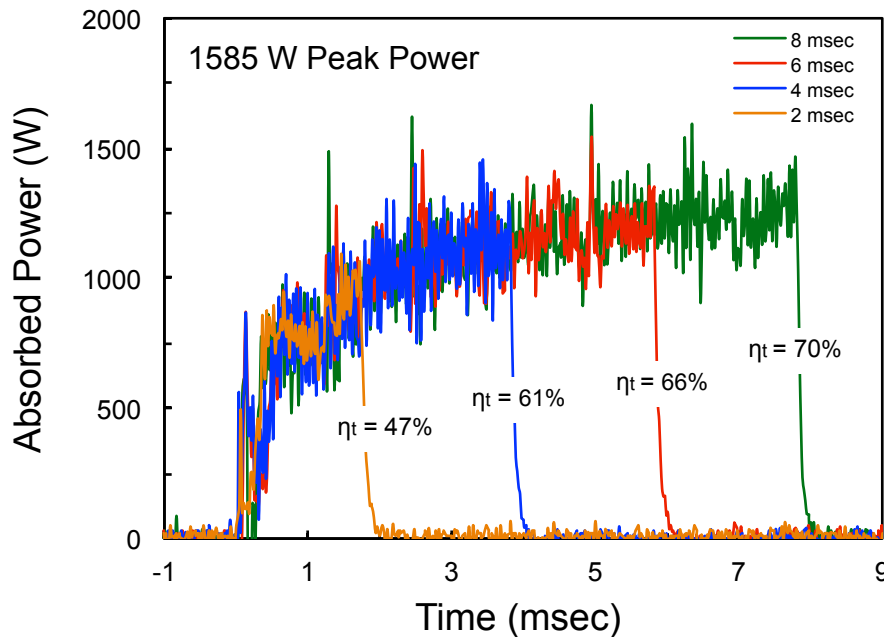
Effect of peak power



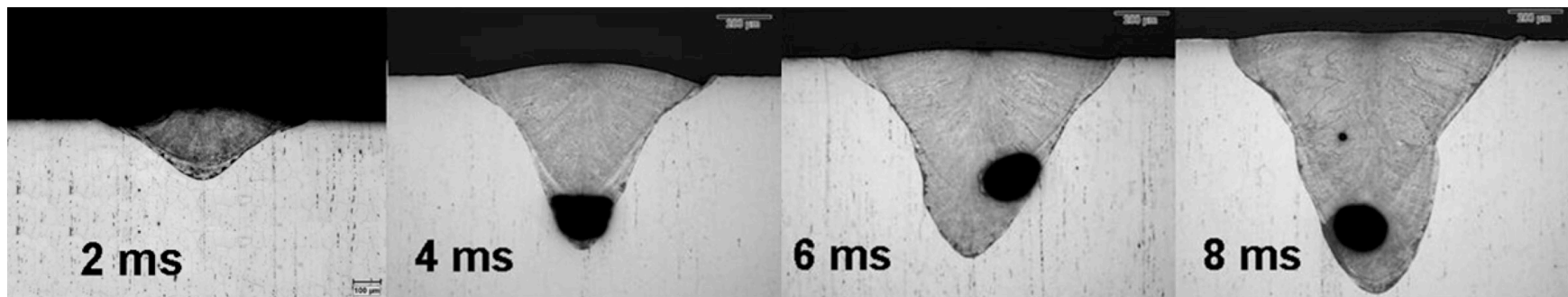
- Initial transfer efficiency about 50%, defines the mode transition and “coupling”
- For low power welds transfer efficiency remains low throughout pulse
- The absorption measurements provide a quantitative description of this evolution



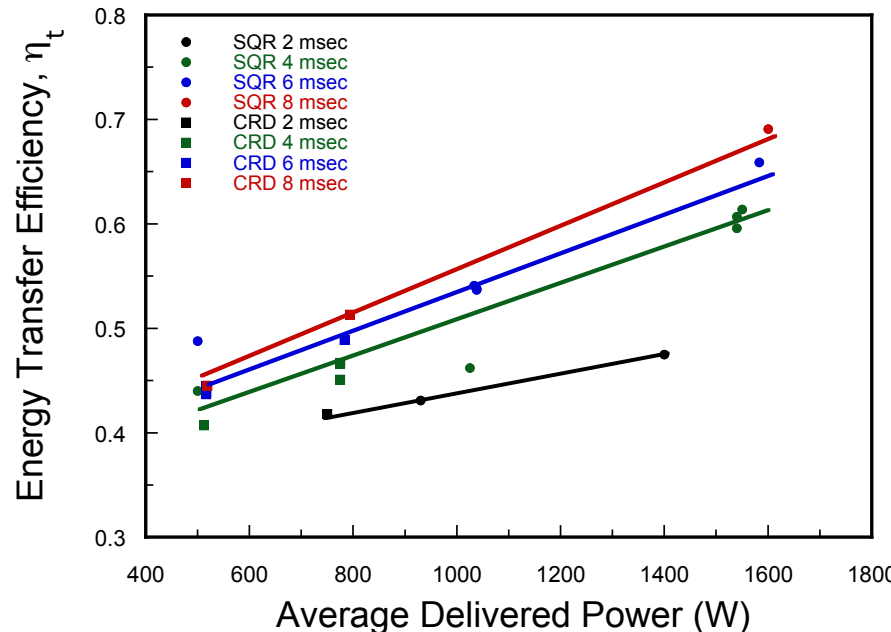
Effect of pulse duration



- Keyhole develops at same initial rate
- Absorption increases logarithmically in time toward a steady value
- Instantaneous transfer efficiency approaches 70%
- Longer time in the high absorption regime increases energy transfer efficiency



Efficiencies and Process Selection

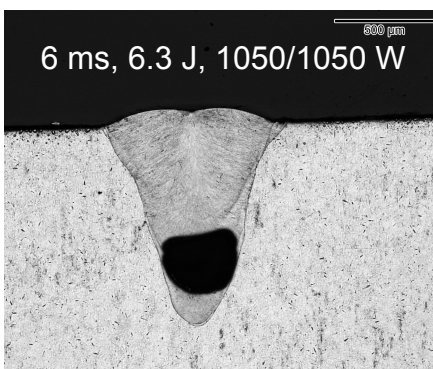
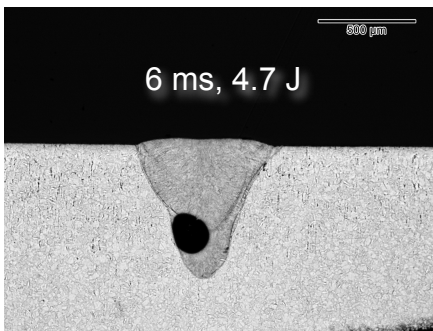
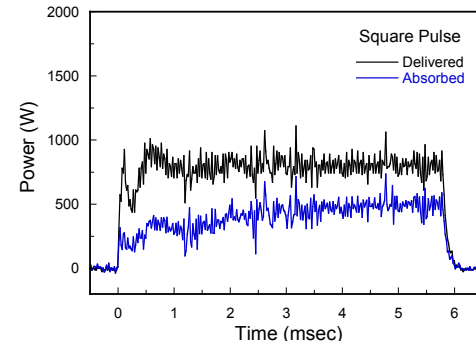


- Higher power pulses generally preferred as they achieve higher energy transfer efficiencies sooner
- Likely to provide a more efficient (lower overall temperature, lower distortion etc.) weld

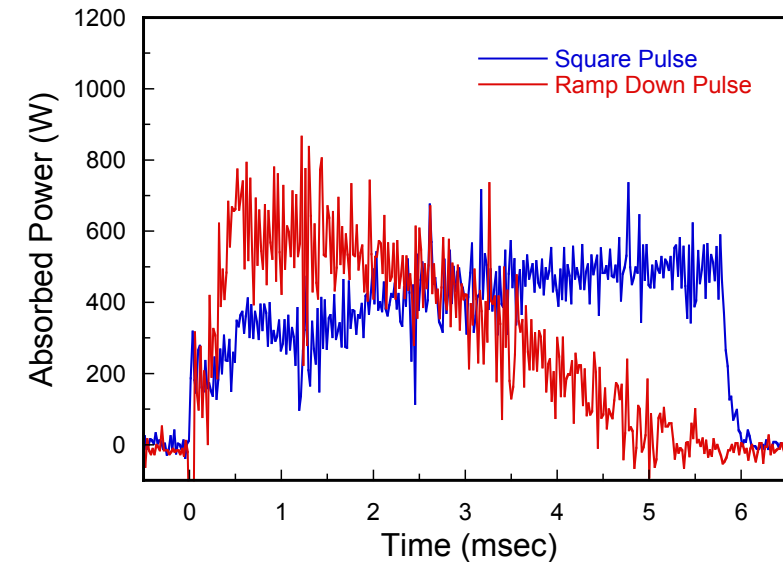
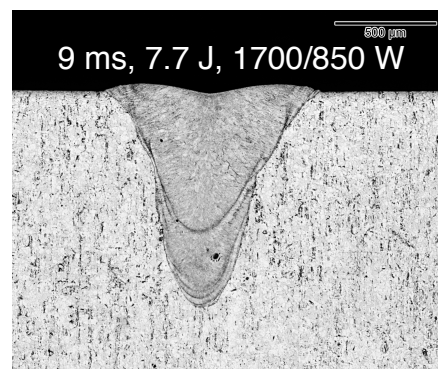
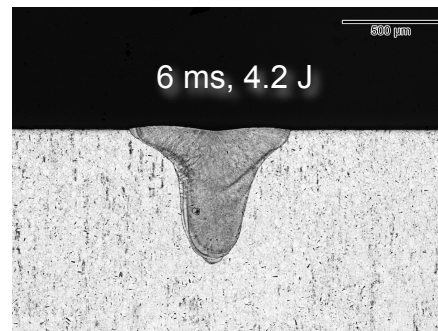
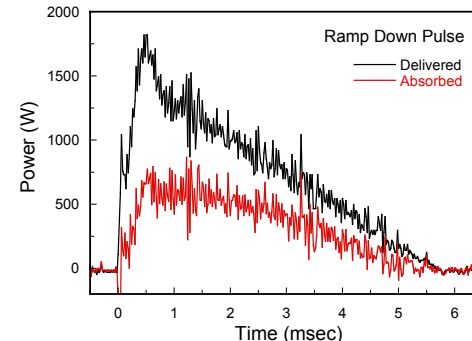
- Transfer efficiency provides a method for assessing temperatures adjacent to spot welds

Pulse shaping

Square Pulse



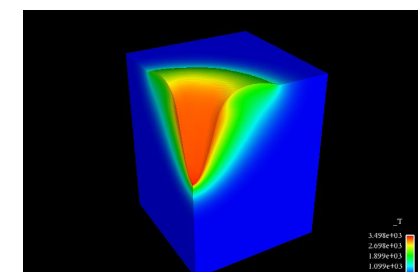
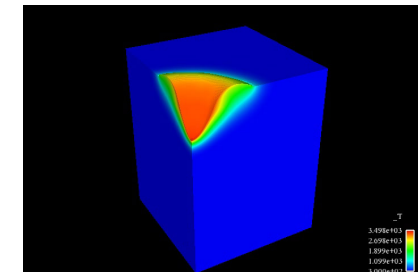
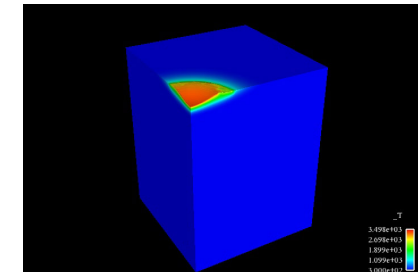
Ramp-Down Pulse



- Pulse shaping allows for gradual collapse of the keyhole, reducing porosity
- Measurements provide an engineering basis to select schedules with respect to penetration, porosity and other thermal constraints

Summary – energy absorption

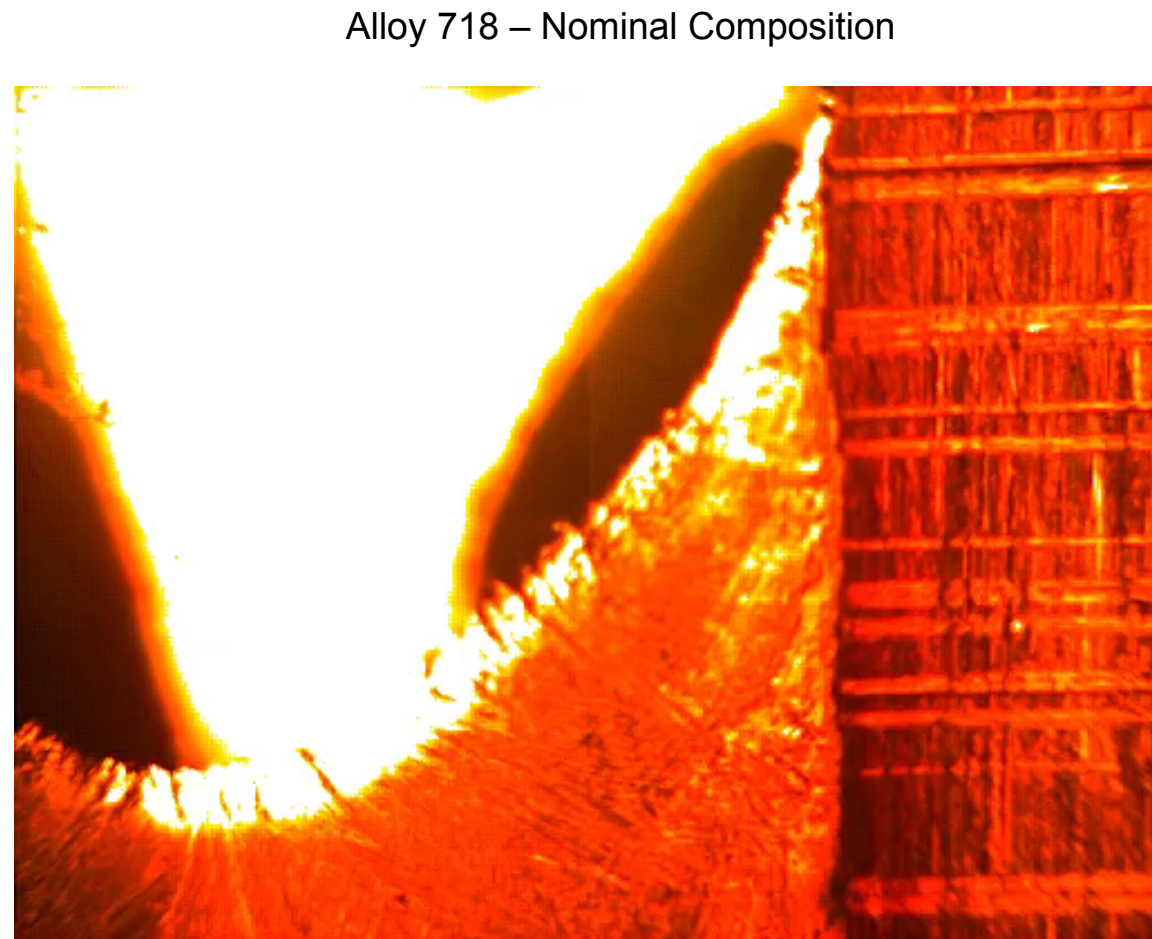
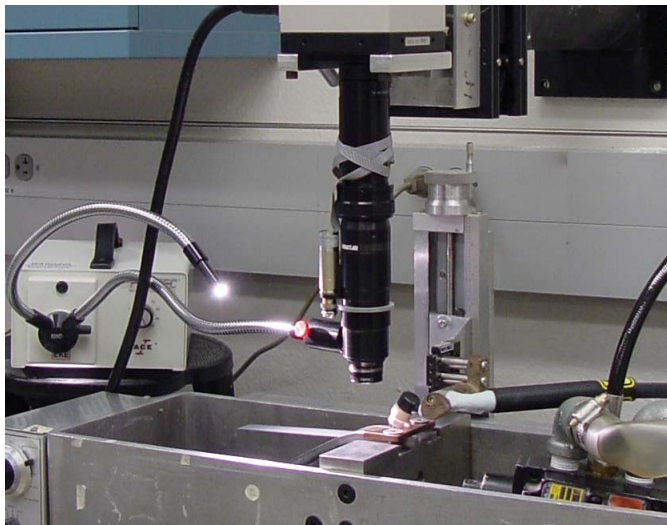
- Energy transfer determinations can be used to estimate welding temperatures, and also reveal important clues about the phenomena associated with the weld pool
- The balance of transfer (and melting) efficiencies can be manipulated with pulse shape, thereby providing a basis for optimization of penetration, defect mitigation, and weld thermal characteristics



- In the next section we look further into the material's response to the process inputs

Hot cracking dynamics in Varestraint testing

- Attempt to gain insight into process/material interactions and cracking
- Varestraint test on IN718 observed by high speed video
- Strain applied to partially molten region of weld



Longitudinal Varestraint test in Alloy 718

- Crack initiates behind S/L interface
- Crack grows in both advancing and retreating directions
- Cracking can be monitored in time

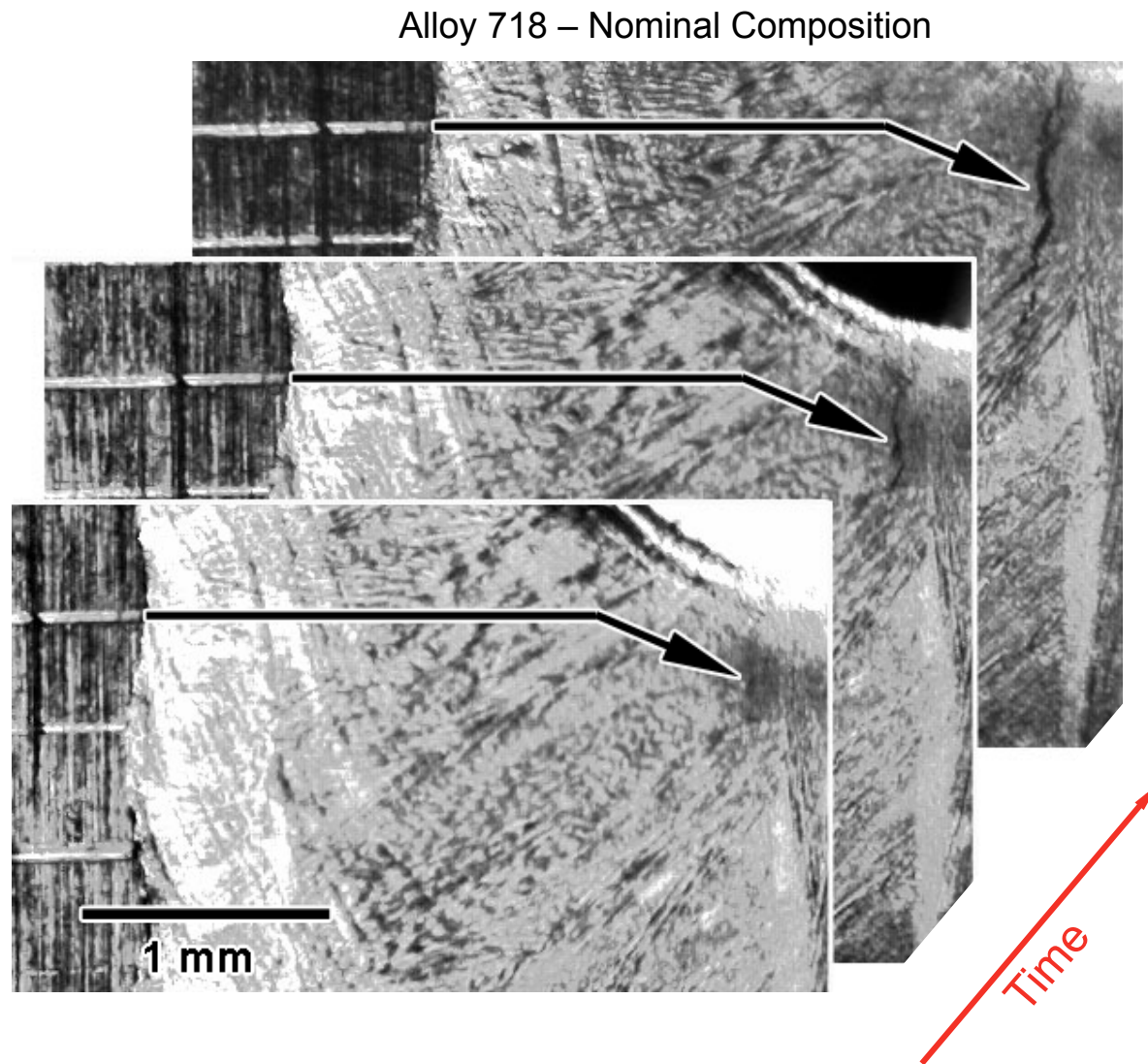
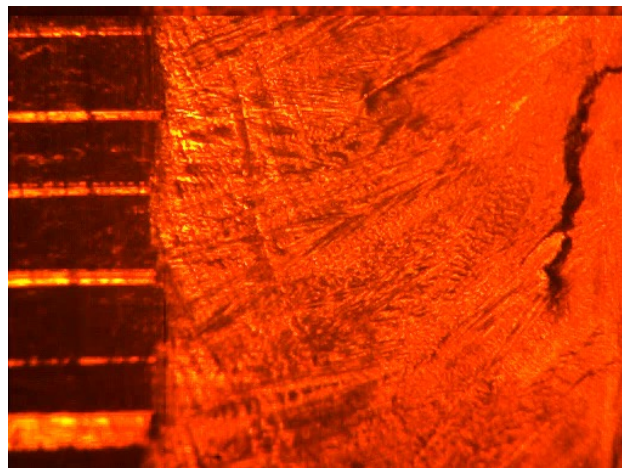
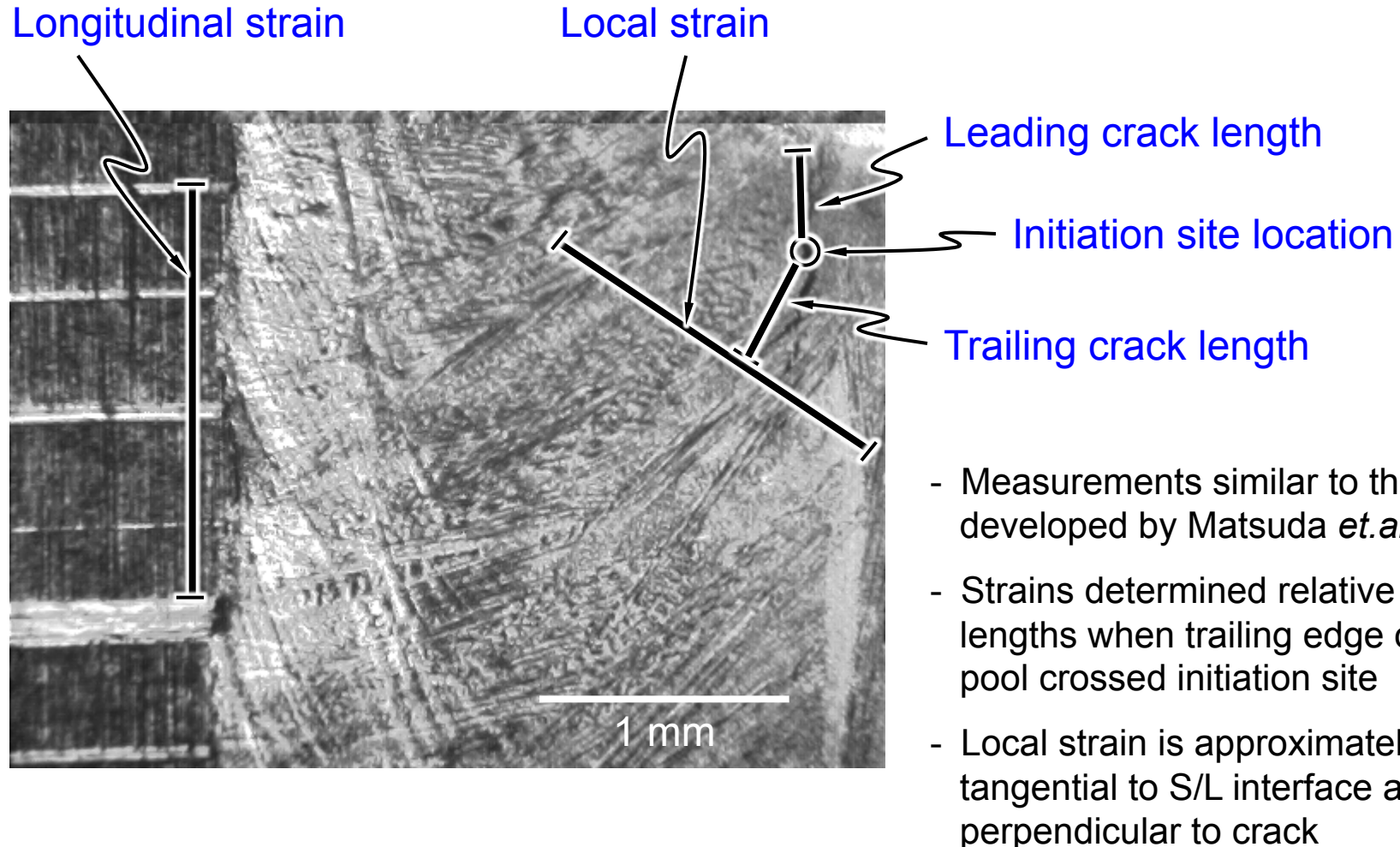
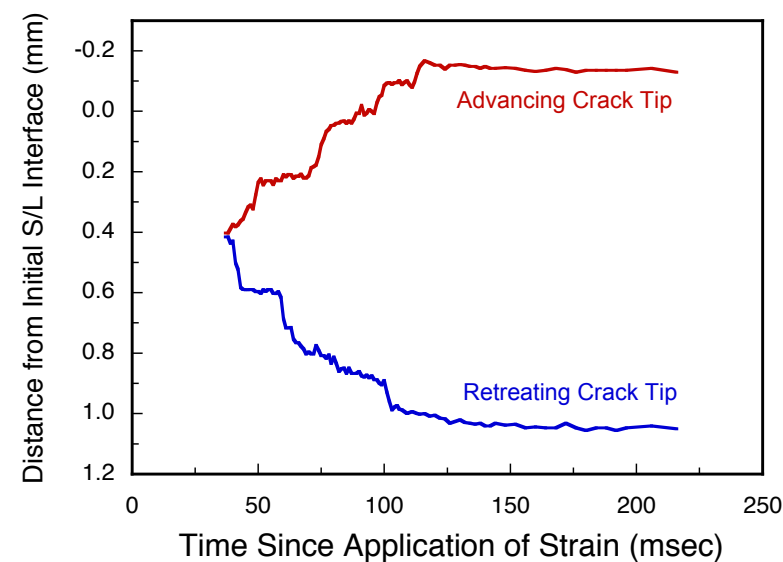
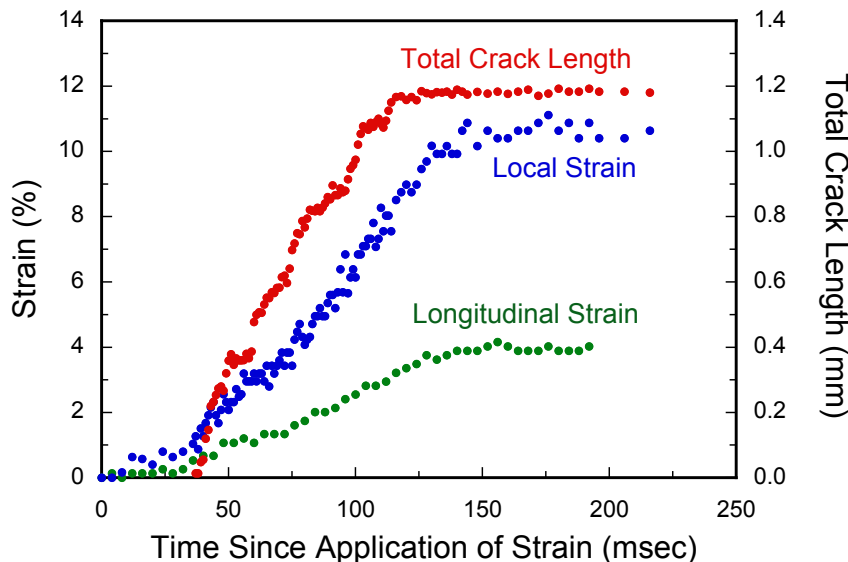


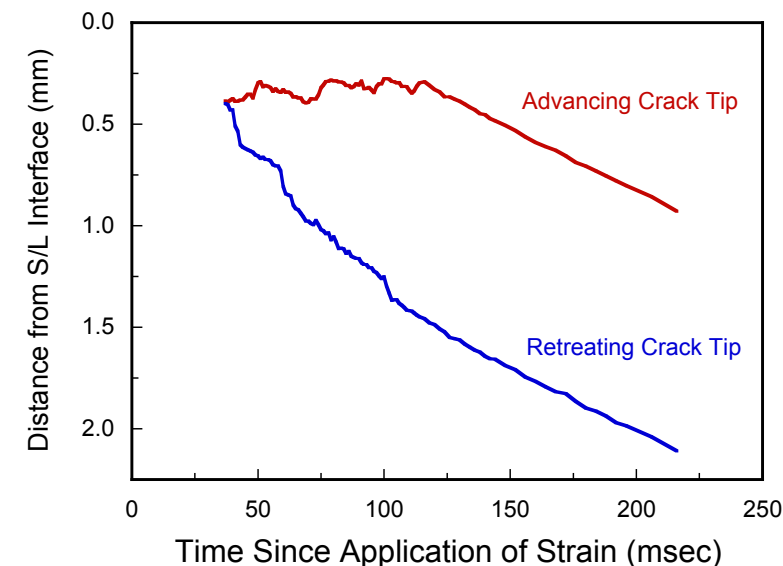
Image measurements



Cracking dynamics

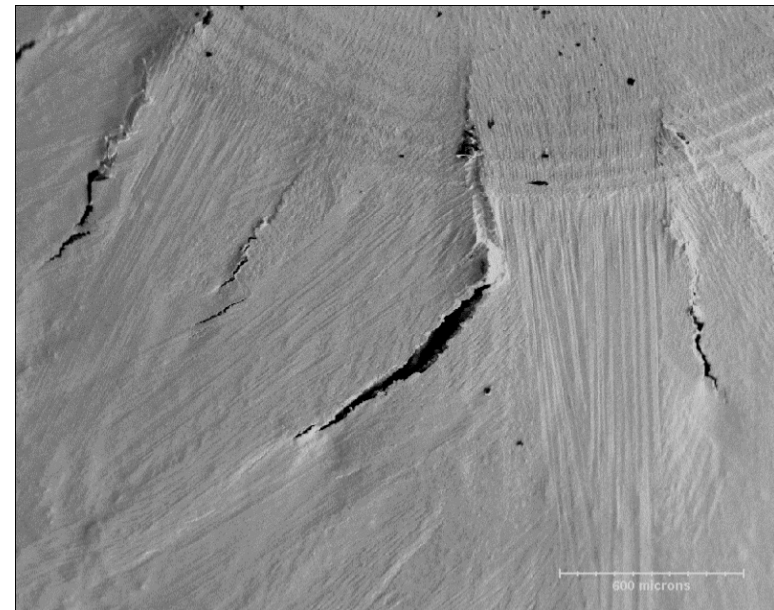
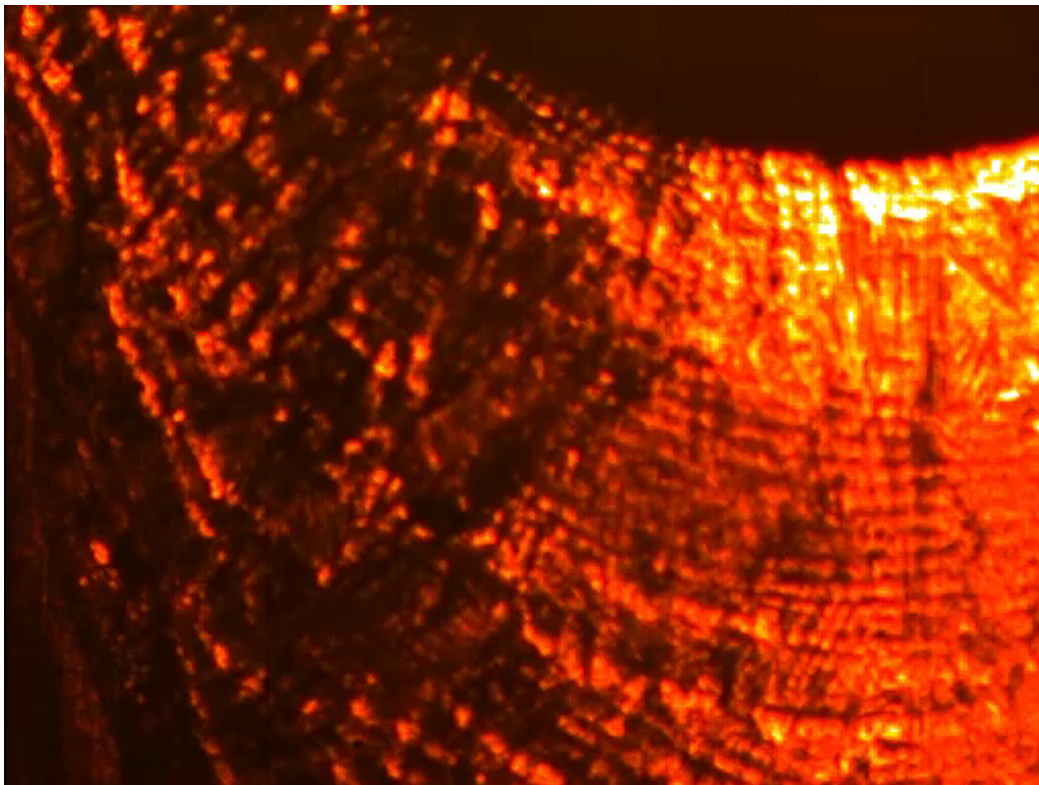


- Cracking initiates at about 1% strain and grows at irregular velocities
- Advancing crack tip moves at the travel speed (i.e. follows an isotherm) like a real hot crack
- Advancing crack tip does not intersect liquidus



Backfilling

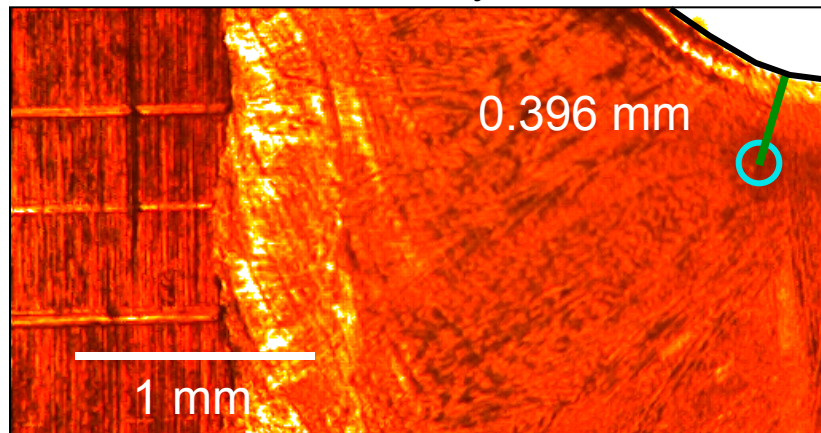
Alloy 718 – High Carbon



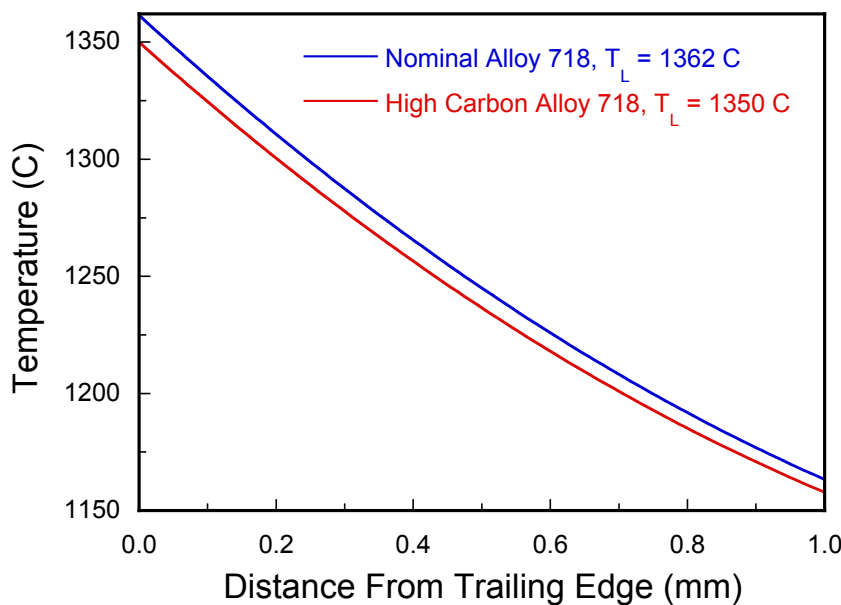
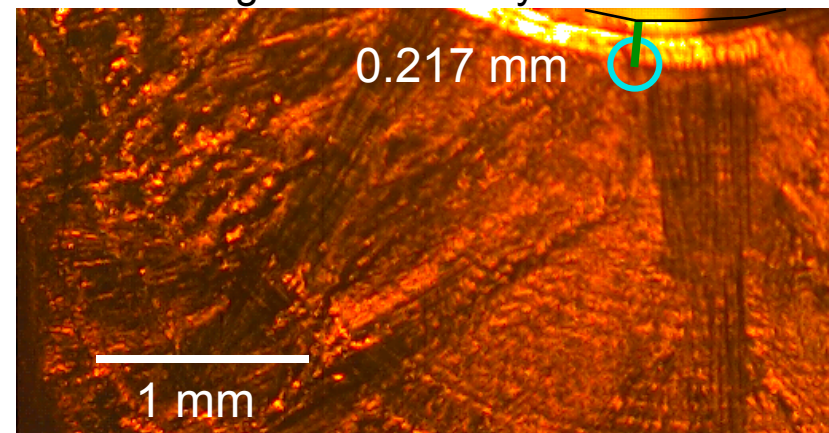
- Backfilling is very difficult to capture optically
- Cracking appears to initiate closer to S/L interface, and to be approximately marked by end of backfilled region
- Frame by frame analysis implies that filling is a continuous event

Crack initiation in Alloy 718

Nominal Alloy 718

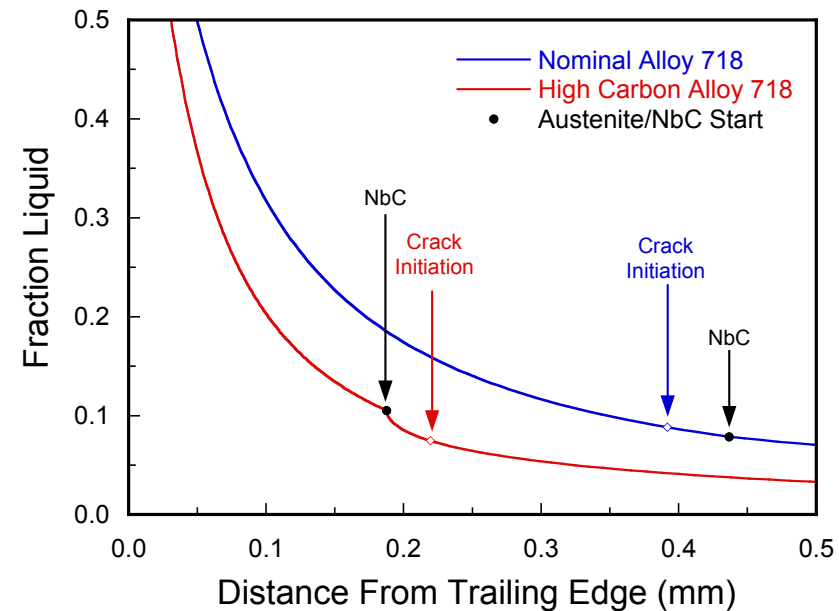
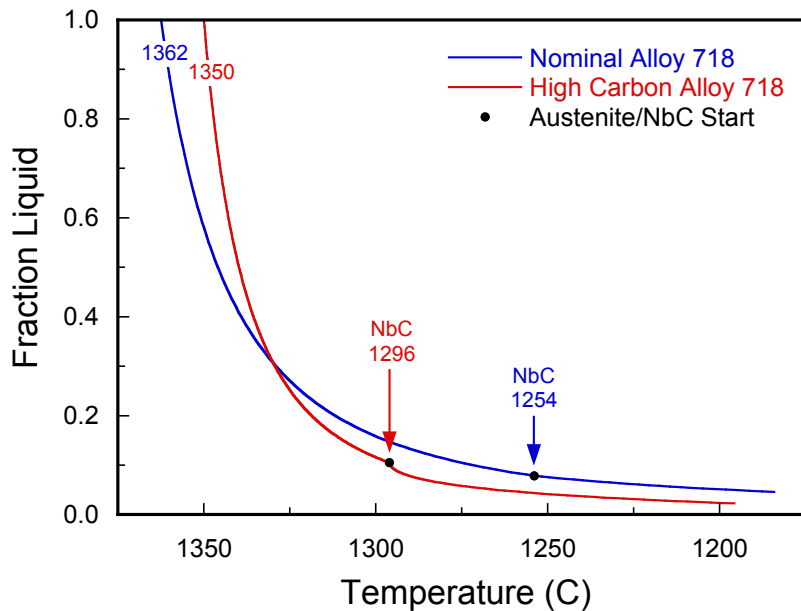


High Carbon Alloy 718



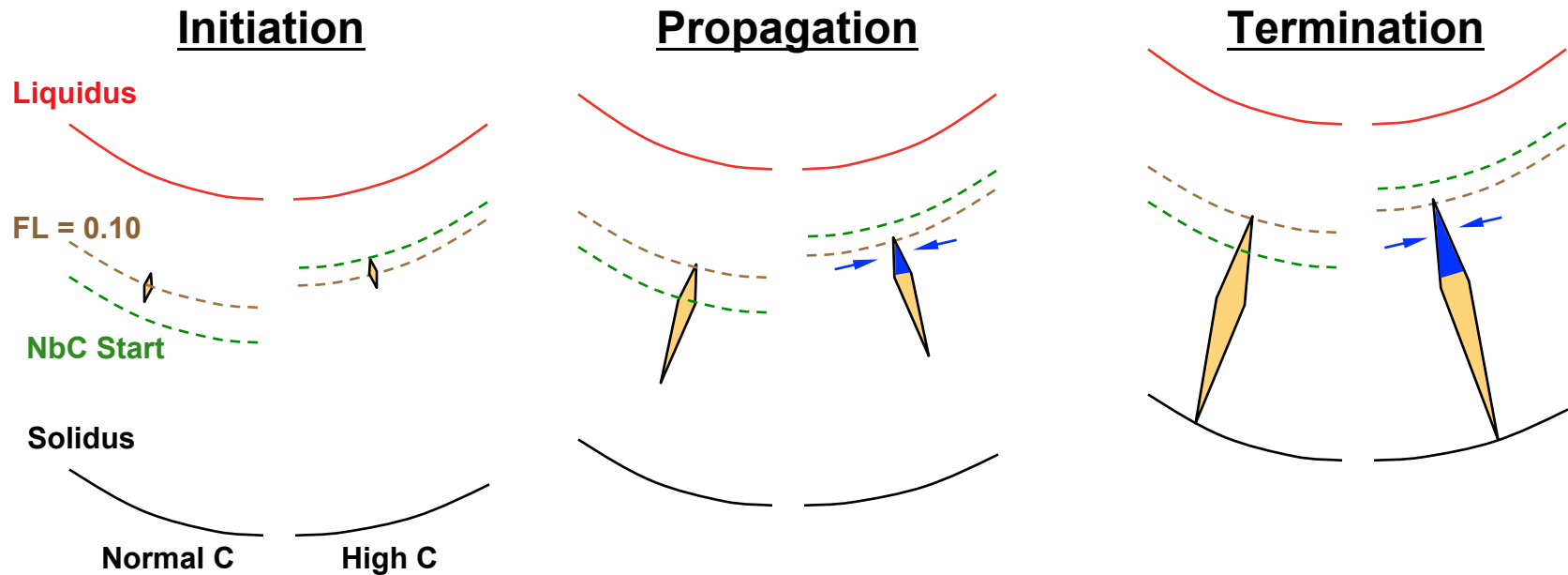
- Temperature associated with crack initiation obtained from video and model estimates

Relationship to fraction liquid



- Crack initiation occurs in the vicinity of 0.10 fraction liquid for both alloys
- Cracks which backfill initiate after eutectic-like reaction starts, consistent with eutectic in backfilled region
- Backfilling appears to be related to interplay of strain development, liquid fraction, and solidification constituent present at advancing opening

Phenomenology



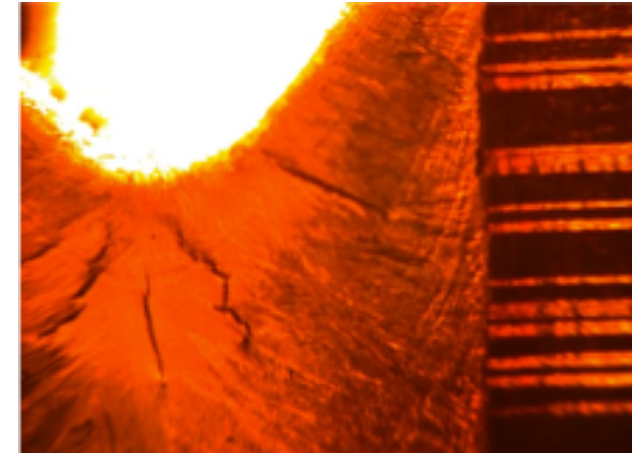
For both unfilled and backfilled solidification cracks:

- Cracking initiates at $\approx 1\%$ local strain and fraction liquid = 0.10
- Forward propagation occurs at approximately constant temperature, and thus constant fraction liquid
- The trailing crack tip propagates in the increasing strain field, and terminates near the solidus

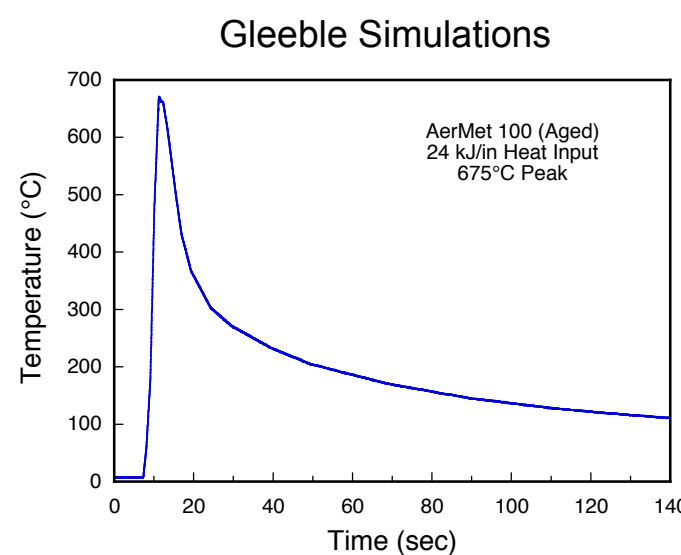
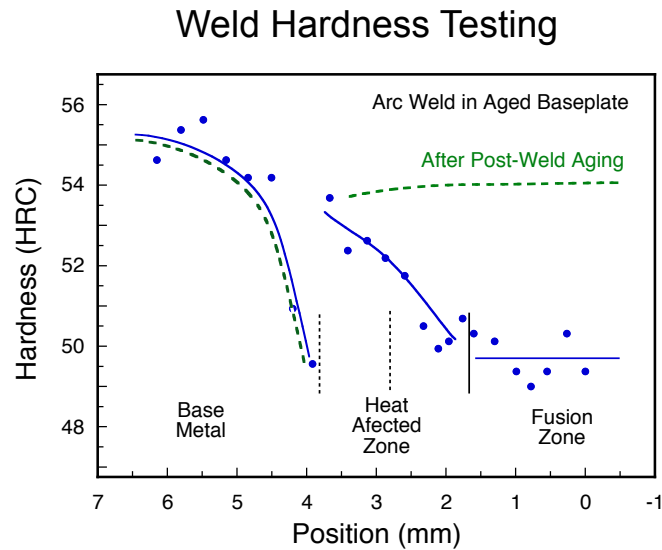
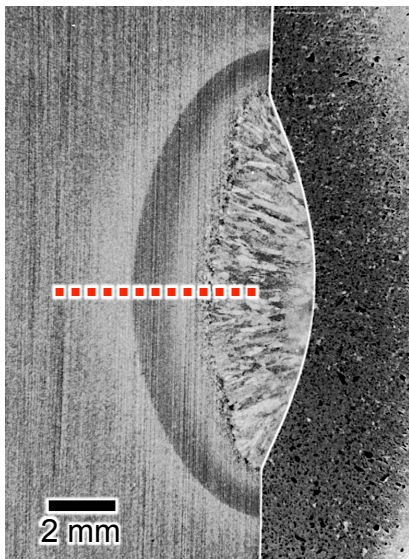
For backfilled solidification cracks, the presence of eutectic composition liquid at the leading opening promotes backfilling, and backfilling appears continuous

Summary - Varestraint cracking

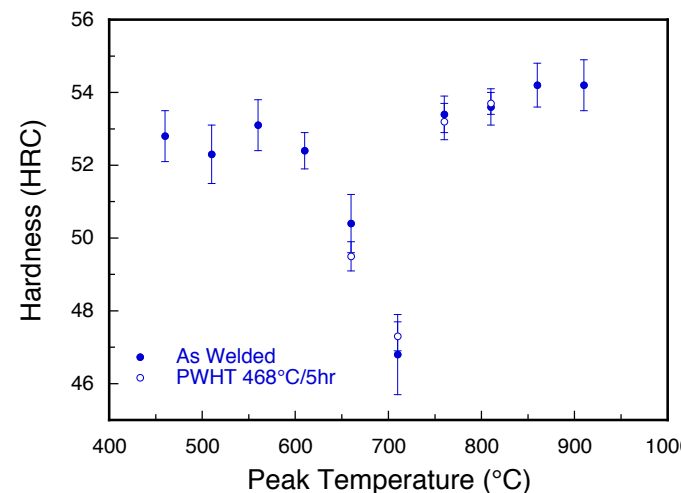
- High speed video analysis coupled with thermal and solidification assessments provide interesting insight into weld cracking phenomenology
- Some potentially useful engineering approximations:
 - Hot cracking in Ni alloys initiates at about 1% local strain and a liquid fraction of about 0.10
 - The advancing crack grows at constant temperature (constant distance behind the pool)
 - For alloys where eutectic initiates ahead of this criteria, backfilling is likely and appears continuous
- In the final section we look at some approximations associated with the development of materials properties in welds



HAZ softening in an ultrahigh strength steel



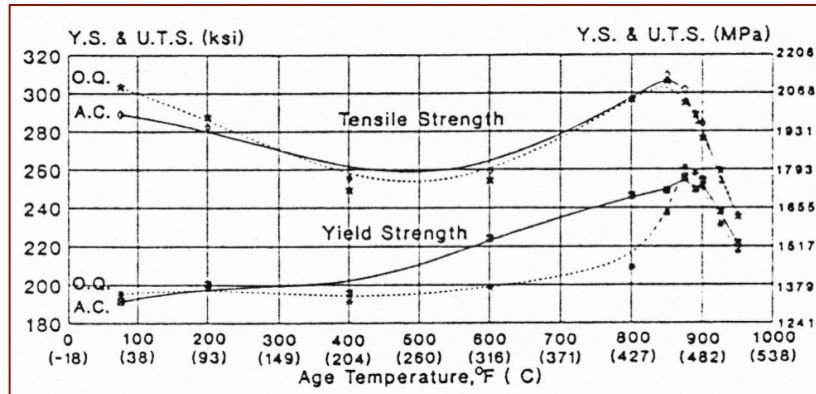
- AerMet 100 is a weldable precipitation hardening Fe-Ni-Co martensitic steel
- Hardness profile in as-welded aged plate shows minima in FZ, near HAZ, and far HAZ
- FZ and near HAZ respond to post-weld aging
- Gleeble simulations replicate this response – hardness minima occurs near 700°C
- What if you don't have a Gleeble?



Goal

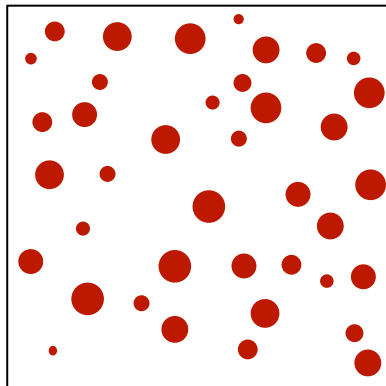
- Handbook or other available data is usually in the form of isothermal heat treatment information
- Not easily adapted to thermal cycles

- Identify a simple analytical approach for estimating the extent of softening



Treatment I.D.	AIR COOL SERIES - PROPERTY SUMMARY (AVERAGE OF DUPLICATE TESTS)								HRC from Charpy Samples**
	Y.S. (ksi)	T.S. (ksi)	% Elong.	% R.A.	K _{IC} (ksi $\sqrt{\text{in}}$)	CVN I.E., (ft-lbs)* R.T.	-65°F	R.T. -65°F	
1	255.8	301.8	16.0	63.9	97.4	28	27.5	54.0	54.0
2	249.3	285.4	15.9	67.4	123.5	36.5	29.5	52.5	52.0
3	252.9	292.0	16.0	65.3	116.1	35	30.5	53.0	53.0
4	247.0	274.4	16.3	69.2	136.7	40.5	30.0	51.0	51.0
5	244.0	265.8	15.5	70.0	144.0	42	31.5	50.0	51.0
6	252.8	298.2	15.6	65.3	94.2	31	27.5	54.0	54.0
7	250.3	286.9	16.6	68.5	119.5	41.5	31.0	52.5	52.5
8	245.9	280.8	16.4	69.5	125.4	41.5	29.0	52.0	52.0
9	250.0	290.8	15.6	67.4	108.0	34.5	27	53.0	52.5
10	242.6	273.2	16.2	70.0	133.2	38.5	26.5	50.5	51.0
11	238.8	267.5	16.1	70.4	140.8	41	27.5	50.0	50.0
24	224.9	241.2	17.3	70.5	151.5+	42	27.5	48.0	47.5
25	232.1	249.5	17.2	72.4	144.6	41	29	48.5	47.5
26	230.9	248.0	16.3	71.6	151.8+	42	27	47.0	47.0
31	251.3	303.6	15.2	61.3	79.2	28.5	26	55.0	55.0
32	252.5	298.3	15.7	63.3	90.6	30.5	28	54.0	54.5
33	248.9	291.1	15.6	63.7	106.5	34	28	54.0	53.0
34	243.5	280.2	15.4	66.1	120.7	37.5	28.5	52.0	51.5
35	248.8	309.4	15.4	61.8	60.3	27	22	55.0	55.0
36	221.5	235.8	18.1	70.3	150.7+	41	25.5	47.0	47.0
37	254.0	284.0	15.3	66.3	127.0	37	30.5	53.0	52.0
38	237.9	254.4	16.1	70.6	147.0	41.5	28.5	49.0	49.5

Overaging microstructure/properties model



Basic Assumptions

- Hardness proportional to shear strength

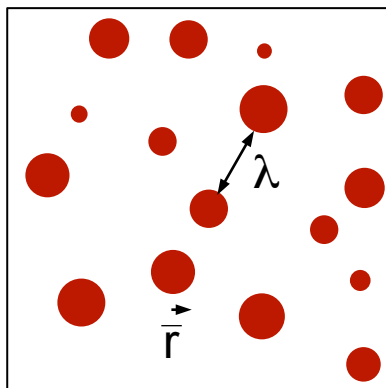
$$H \propto \tau = \frac{\alpha \mu b}{\lambda}$$

$$\lambda \propto \bar{r}$$

$$H \propto \frac{1}{\bar{r}}$$

where:

H = hardness
 τ = shear strength
 α = geometric factor
 μ = shear modulus
 b = burgers vector
 λ = interparticle spacing
 r = particle radius
 For overaging,
 $\lambda \propto r$ (volume fraction constant)



- LSW theory applies for overaging (initial hardening not explicitly considered)

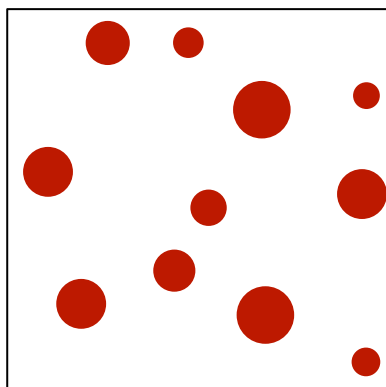
$$\bar{r}_t^3 = \bar{r}_0^3 + Kt$$

$$K = \frac{8}{9} \frac{D\sigma V_m C_\alpha(\infty)}{RT} f(\phi)$$

$$D = D_0 \exp\left(\frac{-Q}{RT}\right)$$

$$K = K_1 \frac{\exp\left(\frac{-Q}{RT}\right)}{T}$$

$$\bar{r}_t^3 = \bar{r}_0^3 + K_1 t \frac{\exp\left(\frac{-Q}{RT}\right)}{T}$$



- Factors other than D are not functions of temperature

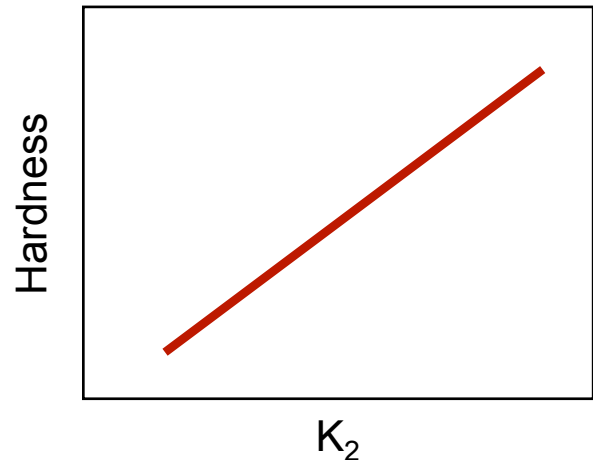
D = diffusivity
 σ = interfacial energy
 V_m = molar volume of ppt
 $C_\alpha(\infty)$ = solubility of solute
 $f(\phi) = 1$ for LSW theory
 R = gas constant
 T = temperature

Coarsening model continued

$$H \propto \frac{1}{\bar{r}} \quad \text{and} \quad \bar{r}^3 = \bar{r}_0^3 + K_1 t \frac{\exp\left(\frac{-Q}{RT}\right)}{T}$$

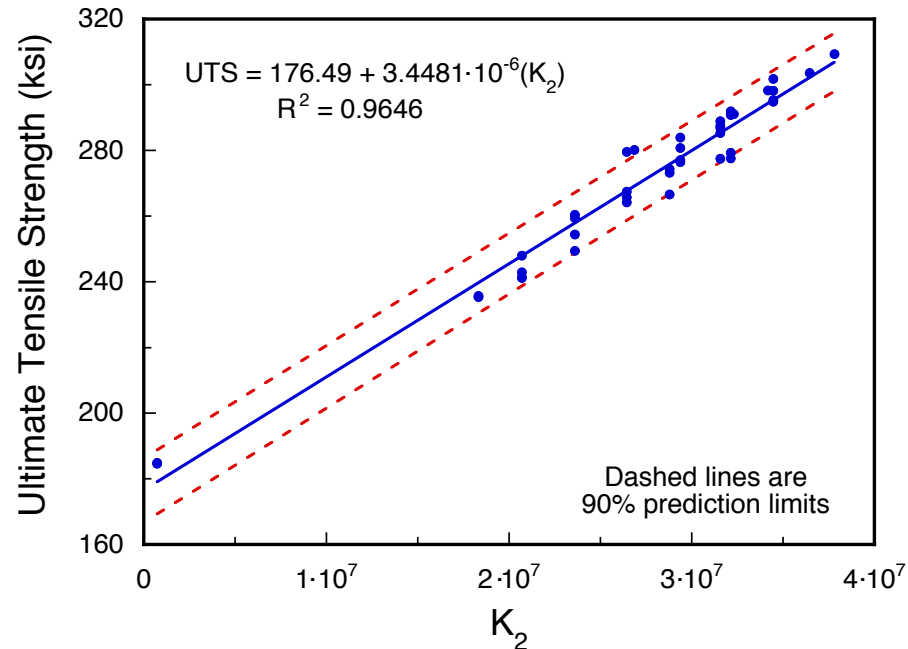
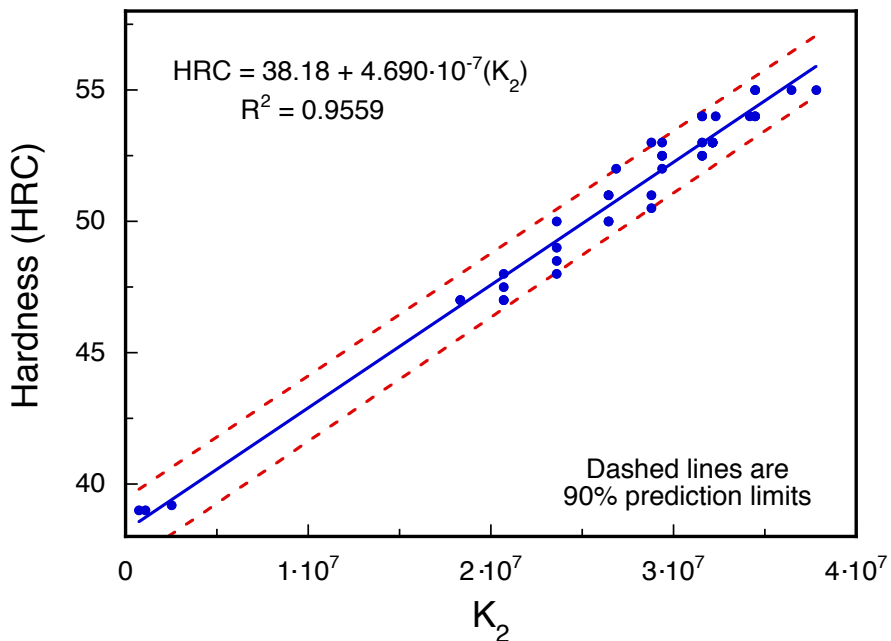
Combining and rearranging leads to:

$$H \propto K_2 \quad \text{where} \quad K_2 = \left(\bar{r}_0^3 + \frac{K_1 t \exp\left(\frac{-Q}{RT}\right)}{T} \right)^{-1/3}$$



- Plot of H versus K_2 should be linear
- Search for r_0 , K_1 , and Q which maximize linearity

AerMet 100 aging correlations



- K_2 parameter linearizes AerMet 100 aging data over a wide range, including peak hardened region
- Can be adapted to complex thermal cycles

Application to non-isothermal cycles

Additivity Rule

$$\int_0^t \frac{dt}{t_a(T)} = 1 \quad \sum_0^t \frac{\Delta t}{t_a(T)} = 1$$

t = time

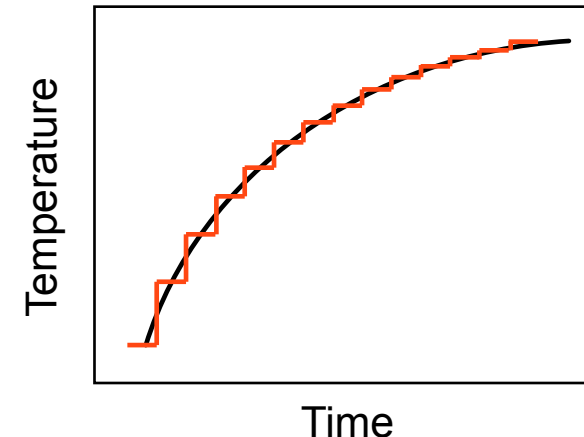
$t_a(T)$ = time to reach a given hardness isothermally

$$H = H_0 + mK_2 = H_0 + m \left(\bar{r}_0^3 + \frac{K_1 t \exp\left(\frac{-Q}{RT}\right)}{T} \right)^{-1/3}$$

H_0 = intercept

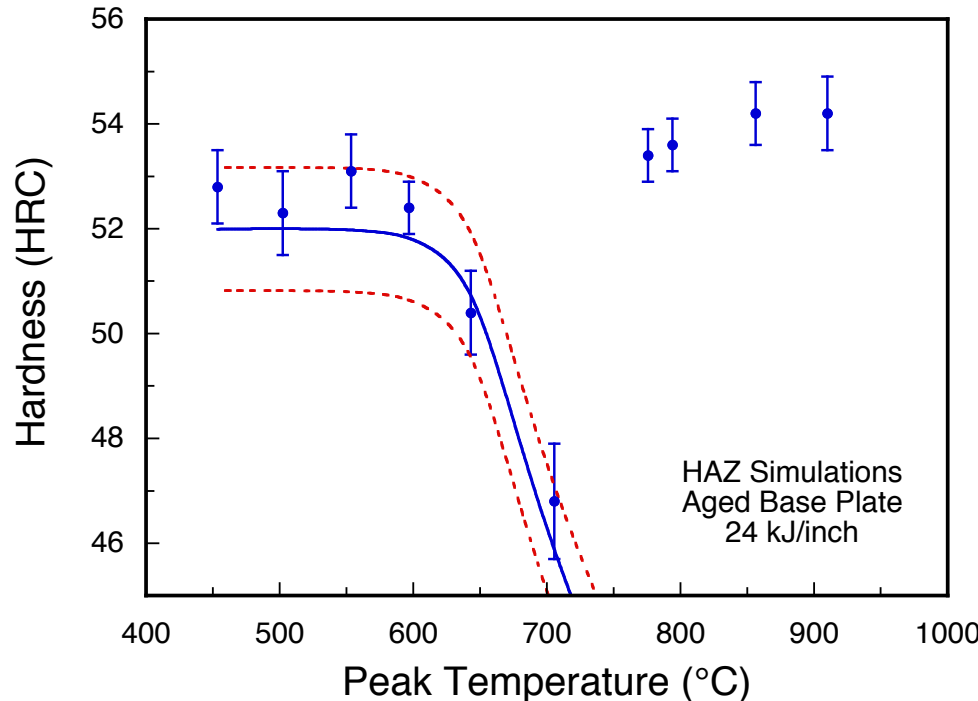
m = slope

$$t = t_a(T) = \frac{T \left[\left(\frac{m}{H - H_0} \right)^3 - \bar{r}_0^3 \right]}{K_1 \exp\left(\frac{-Q}{RT}\right)}$$



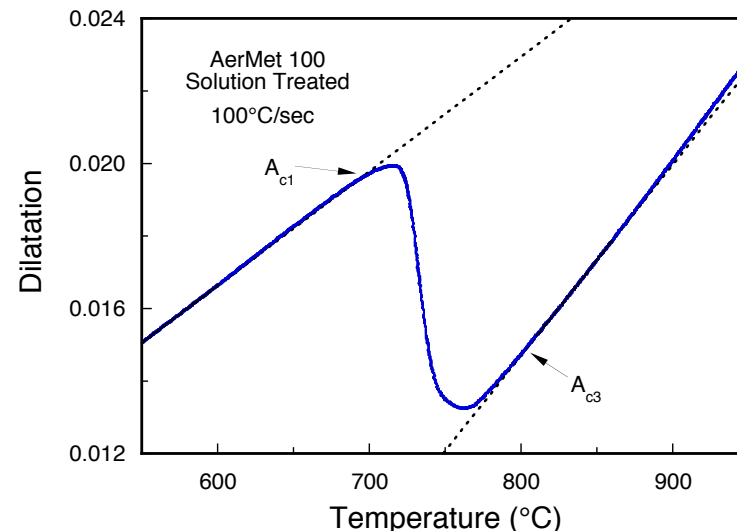
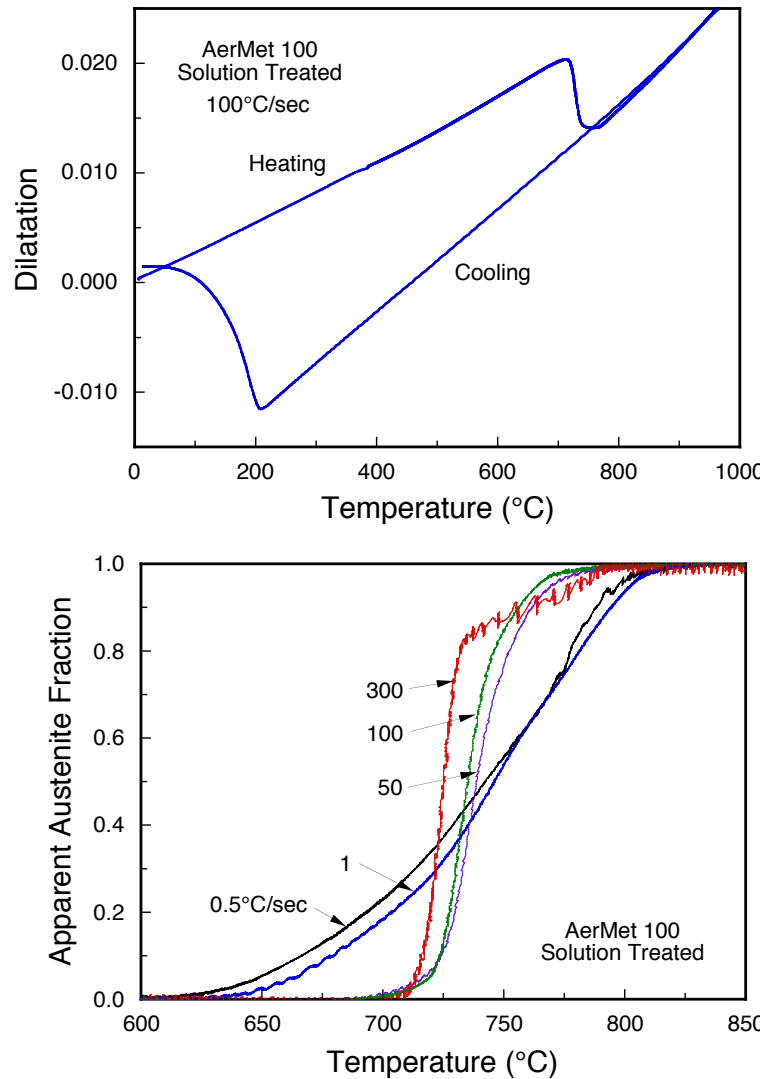
- Time/Temperature path is approximated by isothermal segments
- Goal seeking routine used to find the HRC value which satisfies the summation
- Can also be solved sequentially

Comparison with Gleeble simulations



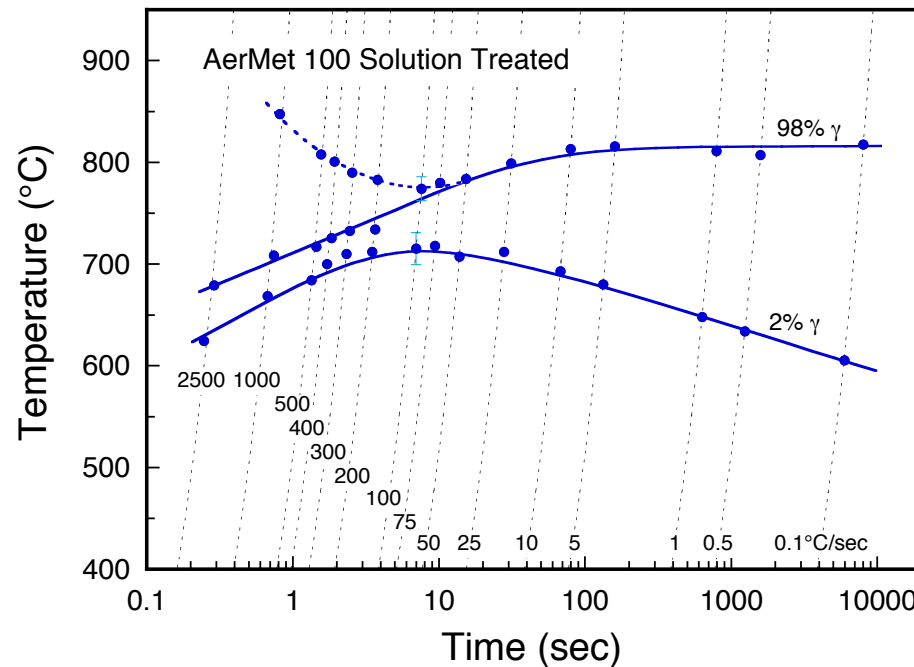
- Additive coarsening model accurately predicts softening in softened region of HAZ
- Cutoff associated with reaustenitization must be determined by another means

Austenitization kinetics



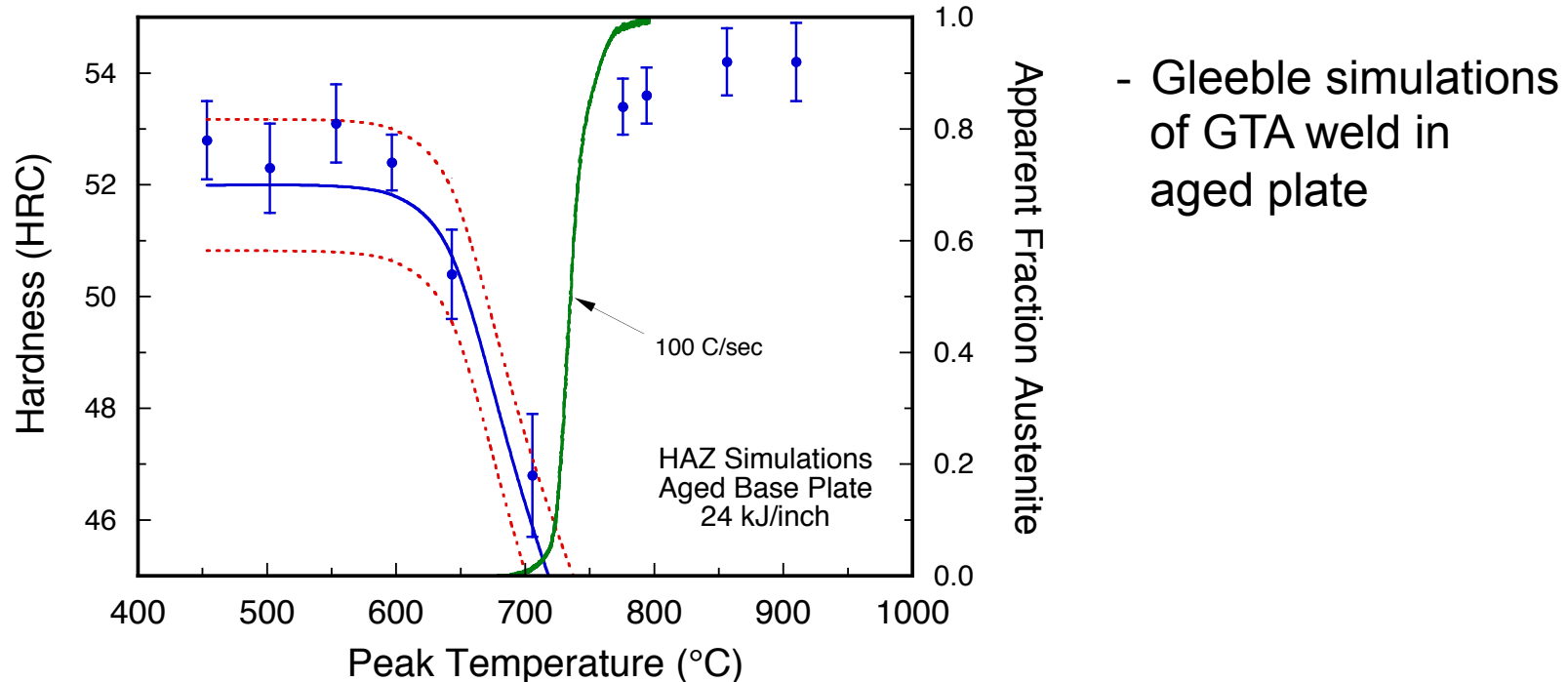
- Dilatometry used to determine transformation temperatures
- Evaluation at different heating rates allows for assessment of transformation kinetics

Continuous heating diagram



- On-heating transformation behavior is complex
- Appears to consist of two distinct heating rate regions
- Solute redistribution appears to be important up to 300-400°C/sec

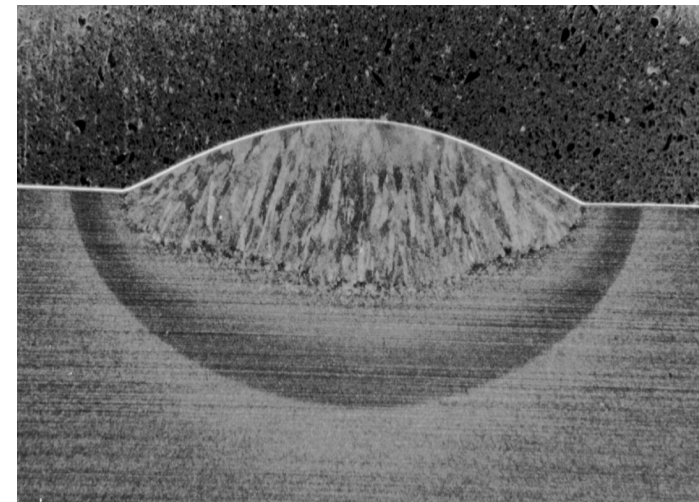
Comparison with Gleeble simulations



- Additive model accurately predicts softening in overaged region of HAZ
- Incorporation of on-heating kinetic data defines bound of softened region

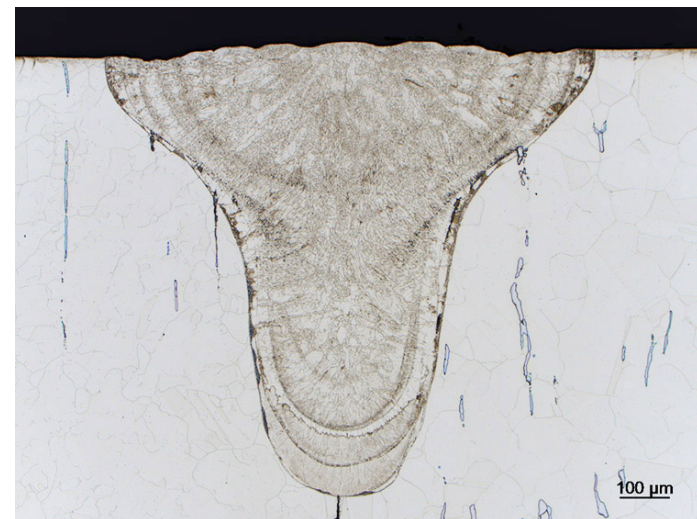
Conclusions – HAZ softening in AerMet 100

- The softened region in AerMet 100 Alloy welds is controlled by overaging and austenite formation
- Weld HAZ softening can be estimated by combination of a simple overaging model and the additivity rule
- Austenite formation in this alloy is complex, dependent on heating rate, and affected by solute redistribution, but can be used to estimate the extent of the softened region



Summary and conclusions

- Many complex dynamic phenomena in welding and welding metallurgy can be reasonably described in comparatively simple engineering terms
- These engineering approximations can provide a bridge between guesswork and more complex simulations or experimental trials, and can help when time and other resources are not available



Acknowledgements



The author acknowledges the many people that have contribute to his continuing education in the field of welding – At the risk of inadvertently neglecting someone and in no particular order, the author express his gratitude for the friendship and support provided by:

John DuPont, Phil Fuerschbach, Mike Maguire, Joe Puskar, Jerome Norris, Don Susan, Mike Cieslak, Mark Reece, Dan MacCallum, Jeff Rodelas, Matt Perricone, Brian Damkroger, Stan Pierce, Paul Moniz, Greg Shelmidine, and Jerry Knorovsky

The encouragement and thoughtful reviews of this manuscript provided by Mike Maguire, Don Susan, and Jeff Rodelas is greatly appreciated.

Sandia National Laboratories is a multi-program laboratory managed and operated by Sandia Corporation, a wholly owned subsidiary of Lockheed Martin Corporation, for the U.S. Department of Energy's National Nuclear Security Administration under Contract DE-AC04-94AL85000.